

Cytotoxic and Noncytotoxic Metabolites from *Teratosphaeria* sp. FL2137, a Fungus Associated with *Pinus clausa*

Chayanika Padumadasa,^{†,‡} Ya-Ming Xu,[†] E. M. Kithsiri Wijeratne,[†] Patricia Espinosa-Artiles,[†] Jana M. U'Ren,[§] A. Elizabeth Arnold,[‡] and A. A. Leslie Gunatilaka^{*,†,§}

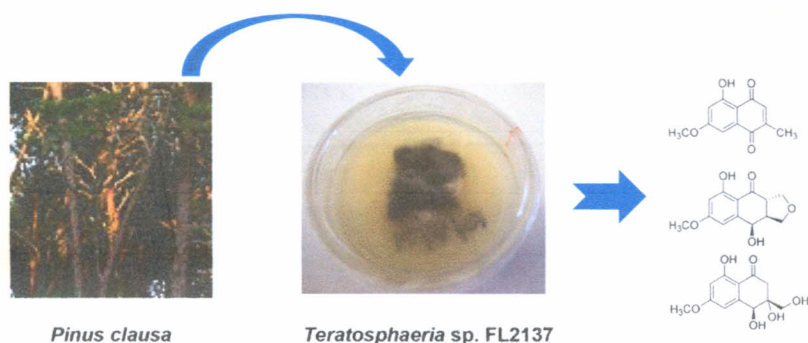
[†]Natural Products Center, School of Natural Resources and the Environment, College of Agriculture and Life Sciences, University of Arizona, 250 E. Valencia Road, Tucson, Arizona 85706, United States

[‡]Department of Chemistry, Faculty of Applied Sciences, University of Sri Jayewardenepura, Gangodawila, Nugegoda, Sri Lanka

[§]Department of Agricultural and Biosystems Engineering, College of Agriculture and Life Sciences, University of Arizona, Tucson, Arizona 85721, United States

[‡]School of Plant Sciences, College of Agriculture and Life Sciences, University of Arizona, Tucson, Arizona 85721, United States

S Supporting Information



ABSTRACT: A new naphthoquinone, teratosphaerone A (**1**), four new naphthalenones, namely, teratosphaerone B (**2**), structurally related to **1**, iso-balticol B (**3**), iso-balticol B-4,9-acetonide (**4**), and (+)-balticol C (**5**), a new furanonaphthalenone, (3aS,9R,9aS)-1(9a),3(3a),9-hexahydromonosporascone (**6**), and the known metabolite monosporascone (**7**) were isolated from *Teratosphaeria* sp. FL2137, a fungal strain inhabiting the internal tissue of recently dead but undecomposed foliage of *Pinus clausa*. The structures of **1**–**6** were elucidated on the basis of their spectroscopic data including 2D NMR, and absolute configurations of **2**, **3**, and **6** were determined by the modified Mosher's ester method. When evaluated in a panel of five tumor cell lines, metabolites **1** and **7** isolated from a cytotoxic fraction of the extract exhibited moderate selectivity for metastatic breast adenocarcinoma cell line MDA-MB-231. Of these, **1** showed cytotoxicity to this cell line with an IC_{50} of $1.2 \pm 0.1 \mu\text{M}$.

Endophytic fungi are important components of plant–microbial ecosystems and represent a rich resource of underexplored biological and chemical diversity.¹ Endophytic fungi inhabiting leaves of forest trees are known to play ecological roles as mutualists,^{2a} as latent pathogens,^{2b} and after leaf death as saprophytic decomposers.^{2c} As part of our continuing search for small-molecule natural products with diverse structures and/or interesting biological activities from endophytic fungi,³ we investigated *Teratosphaeria* sp. FL2137, a fungal strain isolated from dead but undecomposed leaves of *Pinus clausa* (Pinaceae). Many species of the ascomycete genus *Teratosphaeria* are known as widespread foliar pathogens in plants of Proteaceae⁴ and are known to asymptotically infect leaves as endophytes of other plant families.⁵ Historically *Teratosphaeria* species were allied phylogenetically with *Mycosphaerella* (Mycosphaerellaceae), but *Teratosphaeria* is now recognized as a member of the recently established family Teratosphaeriaceae (Ascomycetes).⁶ *Teratosphaeria* is an

understudied genus, and its phylogenetic position remains uncertain.⁴

Teratosphaeria sp. FL2137, when cultured in potato dextrose broth (PDB) containing 0.25 mM CuSO_4 ,⁷ produced six new hexaketide-derived metabolites, teratosphaerones A (**1**) and B (**2**), iso-balticol B (**3**), iso-balticol B-4,9-acetonide (**4**), (+)-balticol C (**5**), and a new furanonaphthalenone, (3aS,9R,9aS)-1(9a),3(3a),9-hexahydromonosporascone (**6**), together with the previously known metabolite monosporascone (**7**). Reported herein are the isolation and structure elucidation of **1**–**7** and cytotoxic activity of **1** and **7** isolated from a cytotoxic fraction of the extract. Although hexaketides structurally related to **1**–**7**, some of which have been shown

Special Issue: Special Issue in Honor of Susan Horwitz

Received: September 30, 2017

Published: January 26, 2018

Table 1. ¹H NMR Data for Compounds 1–6 in CDCl₃ (400 MHz, J in Hz)

position	1	2	3	4	5 ^a	6
1						3.74, t (8.0) 4.04–4.08, m
2	6.73, q (1.6)	2.50, dd (17.6, 4.4), α 2.74, dd (17.6, 10.0), β	2.50, dd (17.6, 4.4), α 2.93, dd (17.6, 10.8), β	2.44, dd (17.4, 4.4) 3.45, dd (17.4, 12.8)	2.60, d (17.2), α 2.90, d (17.2), β	
3		2.36, m	2.41, m	2.09, brd (10.8)		4.04–4.08, m 4.32, dd (8.4, 2.8)
3a						3.21, m
4		4.64, d (2.8)	4.92, d (2.4)	4.90, brs	4.72, s	
5	7.16, d (2.4)	6.46, d (2.4)	6.48, d (2.4)	6.39, s	6.63, d (2.0)	
6						6.34, d (2.4)
7	6.62 (2.4)	6.33, d (2.4)	6.34, d (2.4)	6.39, s	6.32, d (2.0)	
8						6.64, dd (2.4, 1.2)
9	2.14, d (1.6)	1.11, d (6.8)	3.86, m	3.68, brd (12.0), β 4.27, dd (12.0, 2.8), α	3.46, d (11.6) 3.82, d (11.6)	5.19, t (5.2)
9a						3.15, m
11				1.41, s (β-CH ₃)		
12				1.62, s (α-CH ₃)		
3-CH ₃						
5-OH						12.70, s
6-OCH ₃	3.88, s	3.83, s	3.81, s	3.82, s	3.82, s	
7-OCH ₃						3.84, s
8-OH	12.18, s	12.80, s	12.73, s	12.79, s	12.55, s	

^aIn CDCl₃+CD₃OD (50:1).Table 2. ¹³C NMR Data for Compounds 1–6 in CDCl₃ (100 MHz)

position	1	2	3	4	5 ^a	6
1	188.5, C	202.4, C	201.9, C	203.0, C	199.6, C	68.8, CH ₂
2	135.9, CH	40.6, CH ₂	35.6, CH ₂	35.9, CH ₂	44.3, CH ₂	
3	148.7, C	34.4, CH	40.4, CH	33.0, CH	74.5, C	72.4, CH ₂
3a						49.0, CH
4	184.8, C	71.3, CH	70.2, CH	68.2, CH	73.3, CH	200.4, C
4a	133.5, C	146.7, C	145.9, C	142.8, C	145.2, C	109.3, C
5	107.9, CH	107.1, CH	107.4, CH	109.0, CH	109.4, CH	165.7, C
6	165.8, C	166.3, C	166.4, C	166.2, C	166.7, C	99.9, CH
7	106.0, CH	100.4, CH	100.6, CH	101.2, CH	100.1, CH	167.2, C
8	164.0, C	165.6, C	165.6, C	165.4, C	165.0, C	105.5, CH
8a	109.7, C	109.3, C	109.3, C	110.4, C	109.4, C	145.8, C
9	16.4, CH ₃	15.8, CH ₃	64.2, CH ₂	63.4, CH ₂	65.3, CH ₂	67.4, CH
9a						43.5, CH
10				99.4, C		
11				29.8, CH ₃		
12				18.9, CH ₃		
3-CH ₃						
6-OCH ₃	56.0, CH ₃	55.6, CH ₃	55.7, CH ₃	55.7, CH ₃	55.7, CH ₃	
7-OCH ₃						55.7, CH ₃

^aIn CDCl₃+CD₃OD (50:1).

to exhibit antifungal, antiviral, cytotoxic, and DHN (dihydroxynaphthalene) melanin biosynthesis inhibitory activities, have been encountered in species of ascomycete genera,^{9–14} to the best of our knowledge this constitutes the first report of metabolites of a fungus belonging to the genus *Teratosphaeria*.

RESULTS AND DISCUSSION

A preliminary small-scale investigation of *Teratosphaeria* sp. FL2137 to determine culture conditions for optimum production of cytotoxic metabolites indicated that compared to PDB and PDA (potato dextrose agar), PDB containing 0.25 mM CuSO₄ (PDB+Cu²⁺)⁷ provided the highest yield of the

EtOAc extract with cytotoxic activity. Thus, the fungus was cultured in PDB+Cu²⁺ and filtered, and the filtrate extracted with EtOAc. The middle interface layer that existed between EtOAc and H₂O during the extraction and the combined EtOAc extracts were processed separately. Of these, the sample obtained from the interface was found to be responsible for the biological activity of the extract. This was fractionated to afford cytotoxic metabolites 1 and 7. Fractionation of the inactive crude EtOAc extract resulted in the isolation of metabolites 2–7.

Teratosphaerone A (1), obtained as an orange amorphous solid, was determined to have the molecular formula C₁₂H₁₀O₄

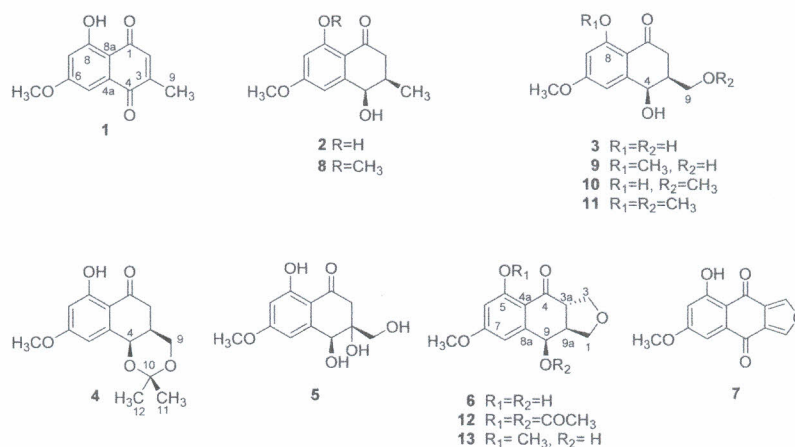


Figure 1. Metabolites 1–7 and their derivatives 8–13.

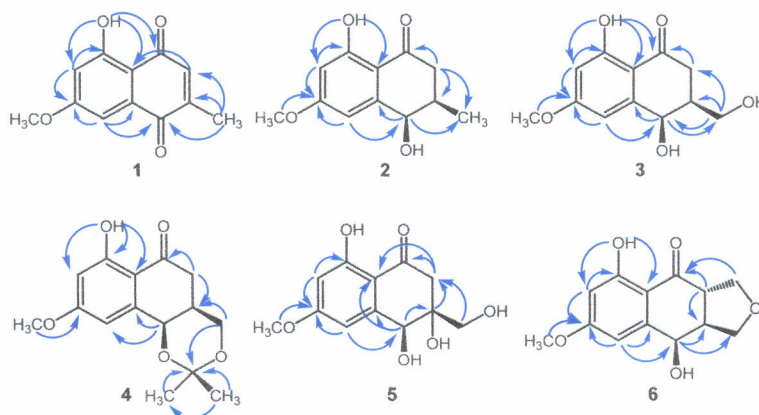


Figure 2. Key HMBC correlations of 1–6.

by a combination of HRESIMS, ¹³C, and HSQC NMR data and indicated eight degrees of unsaturation. Its IR spectrum exhibited absorption bands at 3436, 1645, and 1596 cm⁻¹, indicating the presence of OH, CO, and C=C functionalities. The UV spectrum of **1** exhibited absorption maxima at 218, 268, and 427 nm, typical of a 8-hydroxynaphthoquinone chromophore.¹² Its ¹H and ¹³C NMR data (Tables 1 and 2), assigned with the help of HSQC and HMBC data (Figures S6 and S7, Supporting Information), suggested the presence of a chelated OH [δ_{H} 12.18 (s)], two *meta*-coupled aromatic protons [δ_{H} 6.62 (d, $J = 2.4$ Hz), 7.16 (d, $J = 2.4$ Hz); δ_{C} 106.0, 107.9], a methoxy group [δ_{H} 3.88 (s); δ_{C} 56.0], an olefinic proton [δ_{H} 6.73 (q, $J = 1.6$ Hz); δ_{C} 135.9] that displayed long-range coupling with a methyl group [δ_{H} 2.14 (d, $J = 1.6$ Hz); δ_{C} 16.4], two oxygenated aromatic carbons (δ_{C} 164.0, 165.8), two carbonyl carbons (δ_{C} 184.8, 188.5), and two olefinic carbons (δ_{C} 135.9, 148.7). The analysis of the HMBC data of **1** (Figure 2) confirmed that it contained a naphthoquinone skeleton with CH₃, OCH₃, and OH groups attached to C-3, C-6, and C-8, respectively. On the basis of the foregoing evidence, the structure of teratosphaerone A was established as 8-hydroxy-6-methoxy-3-methyl-1,4-naphthoquinone (**1**).

Metabolites **2–6** were obtained as optically active, colorless amorphous solids. Their spectroscopic data (IR, UV, ¹H and ¹³C NMR) indicated that they contained the basic 3-substituted-6-methoxy-8-hydroxynaphthalen-1(2H)-one carbon

skeleton related to teratosphaerone A (**1**) and balticols A–F.¹⁰ Of these, teratosphaerone B (**2**) displayed a [M + Na]⁺ ion at m/z 245.0786 in its HRESIMS, consistent with the molecular formula C₁₂H₁₄O₄ indicating six degrees of unsaturation. The IR spectrum of **2** exhibited absorption bands at 3429 and 1627 cm⁻¹, suggesting the presence of OH and α,β -unsaturated ketone carbonyl functionalities. Analysis of its ¹H and ¹³C NMR data (Tables 1 and 2) with the help of ¹H–¹H COSY and HSQC data indicated signals due to OH-8 [δ_{H} 12.80 (s); δ_{C} 165.6], H-5 [δ_{H} 6.46 (d, $J = 2.4$ Hz); δ_{C} 107.1], H-7 [δ_{H} 6.33 (d, $J = 2.4$ Hz); δ_{C} 100.4], OCH₃-6 [δ_{H} 3.83 (s); δ_{C} 55.6], and CO (δ_{C} 202.4), confirming the presence of the 6-methoxy-8-hydroxynaphthalen-1(2H)-one moiety in **2**. The NMR data also indicated that it contained two methine groups, of which one is oxygenated [δ_{H} 2.36 (m), 4.64 (d, $J = 2.8$ Hz); δ_{C} 34.4, 71.3], a methylene group [δ_{H} 2.50 (dd, $J = 17.6, 4.4$ Hz), 2.74 (dd, $J = 17.6, 10.0$ Hz); δ_{C} 40.6], and a CH₃ group [δ_{H} 1.11 (d, $J = 6.8$ Hz); δ_{C} 15.8]. The ¹³C NMR spectrum of **2** showed some similarities to that of **1**, except that the resonances due to the olefinic carbons C-2 [δ_{C} 135.9 (CH)] and C-3 [δ_{C} 148.7 (C)] and the carbonyl carbon at C-4 (δ_{C} 184.8) in **1** were replaced in **2** with those at δ_{C} 40.6 (CH₂), 34.4 (CH), and an oxygenated methine carbon at δ_{C} 71.3, respectively. The foregoing suggested that **2** is a tetrahydro analogue of **1** in which the 2(3)-double bond and the carbonyl group at C-4 have undergone reduction. This was confirmed by the

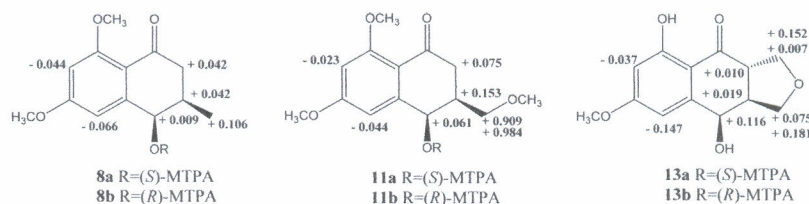


Figure 3. $\Delta\delta$ values [$(\Delta\delta \text{ in ppm}) = (\delta_S - \delta_R)$] obtained for (S)- and (R)-MTPA esters (a and b, respectively) of 8, 11, and 13.

appearance of CH_3 -3 as a doublet [$(\delta_{\text{H}} 1.11 \text{ (d, } J = 6.8 \text{ Hz)})$] in its ^1H NMR spectrum and with the help of the HMBC data (Figure 2), which showed correlations from CH_2 -2 ($\delta_{\text{H}} 2.50, 2.74$) and CH -4 ($\delta_{\text{H}} 4.64$) to CH_3 -3 ($\delta_{\text{C}} 15.8$). The configuration of the α,β -unsaturated cyclohexanone moiety of 2 was deduced by a combination of proton coupling constants and NOE correlations. As the configuration of C-4 was determined to be *R* (see later), the configuration of C-3 was elucidated as *R* from the conformational analysis of energy-minimized conformers of 2 generated by Chem3D (Figure S14, Supporting Information). The large coupling constant (10.0 Hz) between H-3 and one of the protons at C-2 suggested a diaxial orientation of these protons, and the small coupling constant (2.8 Hz) between H-3 and H-4 indicated an equatorial orientation of H-4. This was further supported by NOESY correlations of H-3/H-4 to H₃-9 and of H₃-9/H-4 to H-2, confirming the equatorial orientation of H-4 and CH_3 -9, respectively (Figure S12, Supporting Information). Methylation ($\text{Me}_2\text{SO}_4/\text{K}_2\text{CO}_3/\text{acetone}$) of 2 afforded its monomethyl derivative 8. The absolute configuration of 2 was determined by the application of the modified Mosher's ester method to 8.¹⁵ Reaction of 8 with (R)- and (S)-MTPA-Cl afforded (S)- and (R)-MTPA esters 8a and 8b, respectively. Analysis of $\Delta\delta$ ($\delta_S - \delta_R$) data confirmed the *R* absolute stereochemistry for C-4 (Figure 3). Since NOE data suggested that OH-4 and CH_3 -3 groups are *cis*-oriented (see above), the absolute configuration at C-3 should also be *R*. Thus, the structure of teratosphaerone B was established as (3*R*,4*R*)-3,4-dihydro-4,8-dihydroxy-3-methyl-6-methoxynaphthalen-1(2*H*)-one (2).

Metabolite 3 analyzed for $\text{C}_{12}\text{H}_{14}\text{O}_5$ by a combination of HRESIMS and NMR data. Its IR spectrum showed absorption bands at 3400 and 1625 cm^{-1} , suggesting the presence of OH and α,β -unsaturated ketone carbonyl functionalities. The ^1H and ^{13}C NMR data of 3 closely resembled those of 2 (Tables 1 and 2), but indicated that in 3 the CH_3 -3 [$\delta_{\text{H}} 1.11 \text{ (d, } J = 6.8 \text{ Hz); } \delta_{\text{C}} 15.8$] of 2 has undergone oxidation to a CH_2OH [$\delta_{\text{H}} 3.86 \text{ (m); } \delta_{\text{C}} 64.2$] group. In its HMBC spectrum (Figure 2) CH_2 ($\delta_{\text{H}} 3.86$) of this CH_2OH group showed correlations with C-2 ($\delta_{\text{C}} 35.6$), C-3 ($\delta_{\text{C}} 40.4$), and C-4 ($\delta_{\text{C}} 70.2$), confirming the placement of this group at C-3. Comparison of the ^1H and ^{13}C NMR data of 3 with those of balticol B⁸ suggested that they have the same planar structure with possible dissimilarities in stereoconfigurational disposition of CH_2OH -3 and OH-4, as some major differences were observed for resonances due to C-3 [in 3 $\delta_{\text{C}} 40.4$ (CH); in balticol B $\delta_{\text{C}} 46.0$ (CH)] and H-4 [in 3 $\delta_{\text{H}} 4.92$ (d, $J = 2.4$ Hz); in balticol B $\delta_{\text{H}} 4.70$ (d, $J = 9.3$ Hz)]. The foregoing suggested that 3 is a stereoisomer of balticol B and was designated as iso-balticol B. The relative configuration of balticol B has been determined with the help of coupling constant data for H-3 and H-4, suggesting that CH_2OH -3 is α -oriented and OH-4 β -oriented.¹⁰ However, its absolute configuration is not known. Thus, it was of interest to determine the absolute configuration of these chiral centers in

iso-balticol B (3). As 3 contained OH groups at C-8 and C-9, in addition to that attached to the chiral center (C-4), in order to apply the modified Mosher's ester method¹⁵ for this purpose unambiguously, it was necessary to protect the OH groups at C-8 and C-9. Interestingly, methylation ($\text{Me}_2\text{SO}_4/\text{K}_2\text{CO}_3/\text{acetone}$) of 3 yielded its monomethyl derivatives 9 and 10 and the dimethyl derivative 11 (Figure 1). The ^1H and ^{13}C NMR spectroscopic data of these revealed that the methylation of 3 has taken place at C-8, C-9, and both C-8 and C-9, providing 9, 10, and 11, respectively. Reaction of 11 with (R)- and (S)-MTPA-Cl afforded (S)- and (R)-MTPA esters 11a and 11b, respectively. Analysis of $\Delta\delta$ ($\delta_S - \delta_R$) data confirmed the *R* absolute configuration for C-4 (Figure 3). The configuration of the remaining chiral center (C-3) of 3 was deduced on the basis of NOE correlations (Figure S20, Supporting Information). A strong NOE correlation observed between H-3 and H-4 of 3 suggested that they are cofacial. Thus, the absolute configuration of C-3 was deduced to be *S*. On the basis of the above data, the structure of iso-balticol B was established as (3*S*,4*R*)-3,4-dihydro-4,8-dihydroxy-3-(hydroxymethyl)-6-methoxynaphthalen-1(2*H*)-one (3).

Metabolite 4 exhibited a $[\text{M} + \text{Na}]^+$ ion at m/z 301.1049 in its HRESIMS, consistent with the molecular formula $\text{C}_{15}\text{H}_{18}\text{O}_5$, indicating seven degrees of unsaturation. Its IR spectrum showed an absorption band at 1624 cm^{-1} suggesting the presence of an α,β -unsaturated ketone carbonyl functionality. The ^1H and ^{13}C NMR data of 4 (Tables 1 and 2) assigned with the help of ^1H - ^1H COSY and HSQC data suggested the presence of an aromatic moiety similar to compounds 1–3. However, in 4 the signals of two *meta*-placed aromatic protons appeared as an overlapping signal at $\delta_{\text{H}} 6.39$ in its ^1H NMR spectrum. In addition, the NMR data of 4 demonstrated the presence of two methine groups, of which one is oxygenated [$\delta_{\text{H}} 2.09$ (brd, $J = 10.8$ Hz), 4.90 (brs); $\delta_{\text{C}} 33.0, 68.2$], an oxygenated methylene group [$\delta_{\text{H}} 3.68$ (brd, $J = 12.0$ Hz), 4.27 (dd, $J = 12.0, 2.8$ Hz); $\delta_{\text{C}} 63.4$], a methylene group [$\delta_{\text{H}} 2.44$ (dd, $J = 17.4, 4.4$ Hz), 3.45 (dd, $J = 17.4, 12.8$ Hz); $\delta_{\text{C}} 35.9$], two methyl groups [$\delta_{\text{H}} 1.41$ (s), 1.62 (s); $\delta_{\text{C}} 29.8, 18.9$], a dioxygenated carbon ($\delta_{\text{C}} 99.4$), and a carbonyl carbon ($\delta_{\text{C}} 203.0$). These data indicated the presence of an acetonide moiety in 4, and this was confirmed by the HMBC correlations between the two CH_3 groups and both these CH_3 groups with the dioxygenated carbon (Figure 2). The attachment of this acetonide group was determined to be at C-4 and C-9, as signals due to these carbons appeared relatively downfield ($\delta_{\text{C}} 68.2, 63.4$) in its ^{13}C NMR spectrum and with the presence of an HMBC correlation between one of the CH_2 -9 protons ($\delta_{\text{H}} 3.68$) and C-10 ($\delta_{\text{C}} 99.4$). The presence of an acetonide group in 4 was further confirmed by the occurrence of a peak at m/z 221 corresponding to the fragment ion $[\text{M} - \text{CH}_3\text{COCH}_3 + \text{H}]^+$ in its APCIMS (+) spectrum. The relative configurations of the chiral centers at C-3 and C-4 in 4 were determined with the help of 1D NOESY data (Figure S27, Supporting

Table 3. Cytotoxicity Data of 1 and 7 against a Panel of Selected Tumor Cell Lines^a

compound	cell line ^b				
	NCI-H460	SF-268	MCF-7	PC-3M	MDA-MB-231
1	>5.0	>5.0	3.1 ± 0.2	4.9 ± 0.3	1.2 ± 0.1
7	>5.0	>5.0	>5.0	>5.0	3.8 ± 0.2
doxorubicin	0.4 ± 0.3	0.6 ± 0.1	0.4 ± 0.1	0.2 ± 0.1	0.6 ± 0.2

^aResults are expressed as IC₅₀ values ± standard deviation in μM. Doxorubicin and DMSO were used as positive and negative controls. ^bKey: NCI-H460 = human non-small-cell lung cancer; SF-268 = human CNS cancer (glioma); MCF-7 = human breast cancer; PC-3 M = metastatic human prostate adenocarcinoma; MDA-MB-231 = human breast adenocarcinoma.

Information). A strong NOE correlation between H-4 and H-3 indicated that these protons are cofacial. The above data suggested that 4 is an acetonide derivative of 3 in which acetonide formation has involved the OH groups at C-4 and C-9. The possibility that 4 is an artifact could be ruled out as (i) HPLC investigation of the crude EtOAc extract of *Teratosphaeria* sp. FL2137 clearly indicated the presence of a peak due to 4 (Figure S62, Supporting Information); (ii) acetone was not used in its extraction or purification; and (iii) 3 was resistant to provide 4 even after stirring it in acetone for 7 days at room temperature. Treatment of 3 with acetone in the presence of *p*-TsOH led to slow conversion of it into its acetonide identical with 4, suggesting that it has the same absolute configuration as that of 3. Thus, the structure of metabolite 4 was established as iso-balticol B-4,9-acetonide [(3*S*,4*R*)-8-hydroxy-6-methoxy-10,10-dimethyl-3,4-dihydro-9*H*-naphtho[1,2-*d*][1,3]dioxin-1(2*H*)-one]. It is noteworthy that, although rare, metabolites containing an acetonide group have been reported as natural products.¹⁶

The molecular formula of metabolite 5 was determined to be C₁₂H₁₄O₆ on the basis of its HRESIMS and NMR data, indicating six degrees of unsaturation. Its IR spectrum exhibited absorption bands at 3400 and 1631 cm⁻¹, suggesting the presence of OH and α,β-unsaturated ketone carbonyl functionalities. The ¹H and ¹³C NMR data of 5 (Tables 1 and 2) showed very close similarities to those reported for balticol C [(3*R**,4*S**)-3,4-dihydro-3,4,8-trihydroxy-3-(hydroxymethyl)-6-methoxynaphthalen-1(2*H*)-one].¹⁰ However, balticol C has been reported as a light brown oil with an [α]_D²⁵ of -18.7,⁸ whereas metabolite 5 was obtained as a white amorphous solid with an [α]_D²⁵ of +13.4, suggesting that they are enantiomers. Thus, 5 was designated as (+)-balticol C. The ROESY data of 5 in DMSO-*d*₆ was used to deduce the configuration of CH₂OH-3 (Figure S33, Supporting Information). The presence of a strong NOE correlation between H-4 and OH-3 suggested that they are cofacial. In addition, a NOE correlation was observed between H-4 and H-5, as was reported for balticol C.¹⁰ The foregoing evidence suggested that the relative configurations of the chiral centers C-4 and C-3 are the same as those reported for balticol C.¹⁰ The strong positive Cotton effect at 277 nm observed in the ECD spectrum of 5 (Figure S34, Supporting Information) confirmed the *S* absolute configuration for C-4.¹⁷ Thus, the absolute structure of (+)-balticol C was established as (3*R*,4*S*)-3,4-dihydro-3,4,8-trihydroxy-3-(hydroxymethyl)-6-methoxynaphthalen-1(2*H*)-one (5).

The HRESIMS and ¹H and ¹³C NMR data of metabolite 6 were consistent with the molecular formula C₁₃H₁₄O₅, indicating seven degrees of unsaturation and indicating that it contained an additional carbon atom compared to 1–3 and 5. Its IR spectrum showed absorption bands at 3332 and 1622 cm⁻¹, suggesting the presence of OH and α,β-unsaturated

ketone carbonyl functionalities in 6. The ¹H and ¹³C NMR data of 6 (Tables 1 and 2) assigned with the help of ¹H–¹H COSY and HSQC data established the presence of a chelated OH [δ_{H} 12.70 (s), δ_{C} 165.7], two *meta*-coupled aromatic protons [δ_{H} 6.34 (d, *J* = 2.4 Hz), 6.64 (dd, *J* = 2.4, 1.2 Hz); δ_{C} 99.9, 105.5], and an OCH₃ group [δ_{H} 3.84 (s); δ_{C} 55.7]. The NMR data of 6 also suggested the presence of three methine groups, of which one is oxygenated [δ_{H} 3.15 (m), 3.21 (m), 5.19 (t, *J* = 5.2); δ_{C} 43.5, 49.0, 67.4], two oxygenated methylene groups [δ_{H} 3.74 (t, *J* = 8.0 Hz), 4.06 (m); 4.06 (m), 4.32 (dd, *J* = 8.4, 2.8 Hz); δ_{C} 68.8, 72.4], and a carbonyl carbon (δ_{C} 200.4). The ¹H–¹H COSY data of 6 (Figure S37, Supporting Information) indicated that it contained the cross-coupled spin system CH₂–CH(–CH)–CH–CH₂. Analysis of the HMBC data for 6 (Figure 2) suggested that its structural scaffold is similar to that of monosporascone (7),⁸ a metabolite found to co-occur in this fungal strain (see below). The NMR data indicated that in 6 the carbonyl group at C-9 and the furan ring in 7 have undergone reduction to CHOH and a tetrahydrofuran ring, respectively. The HMBC spectrum demonstrated correlations for H-9 (δ_{H} 5.19) with C-9a (δ_{C} 43.5) and C-1 (δ_{C} 68.8), H₂-3 (δ_{H} 4.04–4.08 and 4.32), and H-3a (δ_{H} 3.21) with C-4 (δ_{C} 200.4). Acetylation (Ac₂O/pyridine) of 6 afforded its diacetate 12, whereas methylation (Me₂SO₄/K₂CO₃/acetone) yielded the monomethyl derivative 13 (Figure 1), confirming that 6 contained two OH groups, of which one is phenolic. The downfield shift of H-9 in the diacetate 12 suggested that the free OH group in 13 is at C-9. The absolute configuration of C-9 was determined by the application of the modified Mosher's ester method to the monomethyl derivative 13.¹⁵ Reaction of 13 with (*R*)- and (*S*)-MTPA-Cl afforded (*S*)- and (*R*)-MTPA esters 13a and 13b, respectively. Analysis of $\Delta\delta$ (δ_{S} – δ_{R}) data confirmed the *R* absolute stereochemistry for C-9 (Figure 3). The relative configuration of C-9a of 6 was deduced on the basis of its 1D NOESY data (Figure S40, Supporting Information). Irradiation of H-9 of 6 led to a significant enhancement of H-9a, suggesting that these protons are cofacial and the *S* absolute configuration for C-9a. Although in 6 no significant enhancement of H-3a was observed upon irradiation of H-9, irradiation of H-9a of its monomethyl derivative 13 led to a significant enhancement of H-9, suggesting *trans*-(C-9a–C-3a) ring fusion in 13. On the basis of the above data, the structure of metabolite 6 was deduced as (3*aS*,9*R*,9*aS*)-1(9*a*),3(3*a*),9-hexahydromonosporascone [(3*aS*,9*R*,9*aS*)-5,9-dihydroxy-7-methoxy-3,3*a*,9,9*a*-tetrahydronaphtho[2,3-*c*]furan-4(1*H*)-one].

Metabolite 7 was identified as monosporascone (5-hydroxy-7-methoxy-4,9-dioxonaphtho[2,3-*c*]furan) by comparison of its NMR data with those reported.^{8,12}

Metabolites 1 and 7 isolated from the cytotoxic fraction of the extract were evaluated for *in vitro* cytotoxic activity using the resazurin-based colorimetric (Alamar Blue) assay¹⁸ against

a panel of five tumor cell lines, NCI-H460 (human non-small-cell lung cancer), SF-268 (human CNS cancer; glioma), MCF-7 (human breast cancer), PC-3 M (metastatic human prostate adenocarcinoma), and MDA-MB-231 (human breast adenocarcinoma). As presented in Table 3, teratosphaerone A (**1**) exhibited selective cytotoxic activity against MDA-MB-231 (IC_{50} $1.2 \pm 0.1 \mu\text{M}$) and moderate activity against MCF-7 and PC-3M, but had no activity against NCI-H460 and SF-268 cell lines up to a concentration of $5.0 \mu\text{M}$. Metabolite 7 showed similar selectivity to the MDA-MB-231 cell line with moderate cytotoxicity (IC_{50} $3.8 \pm 0.2 \mu\text{M}$) and no activity against NCI-H460, SF-268, MCF-7, and PC-3 M cell lines up to a concentration of $5.0 \mu\text{M}$.

EXPERIMENTAL SECTION

General Experimental Procedures. Optical rotations were measured in MeOH with a Jasco Dip-370 digital polarimeter. UV spectra were recorded using a Shimadzu UV-1601 UV-vis spectrophotometer in EtOH. IR spectra were recorded on a Shimadzu FTIR-8300 spectrometer using samples prepared in KBr discs. ECD spectra were recorded in MeOH on a Jasco 810 spectrometer at 25°C , using a quartz cell with 1.0 mm optical path length. 1D and 2D NMR spectra were recorded in CDCl_3 (unless otherwise stated) with a Bruker Avance III 400 spectrometer at 400 MHz for ^1H NMR and 100 MHz for ^{13}C NMR using residual CHCl_3 as an internal reference. Low-resolution and high-resolution MS were recorded on a Shimadzu LCMS-QP8000 α and an Agilent G6224A TOF mass spectrometer, respectively. Preparative HPLC separations were performed on a Waters Delta Prep 4000 preparative chromatography system equipped with a Waters 996 photodiode array detector and a Waters Prep LC controller utilizing Empower Pro software and using an RP column (Phenomenex Luna 5 μm , C_{18} , 100 \AA , $250 \times 10 \text{ mm}$); chromatograms were acquired at 254 and 270 nm. Column chromatography was performed using silica gel (40 μm ; J. T. Baker). Analytical and preparative thin layer chromatography (TLC) were carried out using precoated 0.25 mm thick plates of silica gel 60 F_{254} (Merck). Compounds on analytical TLC were visualized under UV light and/or by spraying anisaldehyde followed by heating.

Fungal Isolation and Identification. In March 2008, newly senesced leaves (i.e., needles) of a living individual of *Pinus clausa* were obtained from a branch ca. 1.25 m above the ground of a pine-dominated scrub forest at Archbold Biological Station in Florida, USA ($27^\circ 11' 19'' \text{N}$, $81^\circ 20' 15'' \text{W}$, ca. 35 m.a.s.l.) as part of a larger study of fungal diversity.¹⁹ Each needle was washed in tap water and then cut into 96 segments (each ca. 2 mm^2). Segments were surface-sterilized by agitating for 30 s in 95% EtOH, 2 min in 0.5% NaOCl, and 2 min in 70% EtOH.¹⁹ Segments were allowed to surface-dry under sterile conditions and then were placed singly onto 2% malt extract agar (MEA) in individual 1.5 mL micro centrifuge tubes. Tubes were sealed with Parafilm and incubated at room temperature (ca. 21.5°C) under ambient light/dark conditions for one year. Emergent fungi were isolated on 2% MEA, vouchered in sterile water, and deposited as living vouchers at the Robert L. Gilbertson Mycological Herbarium at the University of Arizona. Of these, the strain FL2137 was selected for this study. Total genomic DNA was isolated from fresh mycelium as described previously.¹⁹ The nuclear ribosomal internal transcribed spacers and 5.8s gene (ITS rDNA; ca. 600 base pairs [bp]) and the first ca. 600 bp of the nuclear ribosomal large subunit (LSU rDNA) were PCR-amplified as a single fragment.¹⁹ The amplicon was sequenced bidirectionally as described previously.¹⁹ A consensus sequence was assembled, and basecalls were assigned *phred*²⁰ and *phrap*²¹ in Mesquite,²² followed by manual editing in Sequencher (Gene Codes Corp.). Because the isolate did not produce diagnostic fruiting structures in culture, three approaches were used to identify FL2137 using molecular sequence data. First, the entire sequence was compared against GenBank via BLASTn.²³ BLAST results placed the strain in the Dothideomycetes with high similarity to diverse Capnodiales (including unidentified endophytes as well as described

species of *Teratosphaeria* and relatives). Next, the sequence was evaluated using the naïve Bayesian classifier for fungi²⁴ available through the Ribosomal Database Project (<http://rdp.cme.msu.edu/>). Comparison with the UNITE Fungal ITS Trainset and RDP Classifier Fungal 28S Trainset 11 (ITSrDNA and LSUrDNA portions, respectively) placed the strain in the Capnodiales but could not place it to a finer taxonomic level. Therefore, a phylogenetic approach was used to identify FL2137. Examination of BLAST results revealed potential placement within *Teratosphaeria*, with top matches including several taxa evaluated phylogenetically in a previous study.²⁵ The ITSrDNA portion of the sequence was integrated into the publically archived sequence alignment, and the data set was aligned automatically in MUSCLE (<http://www.ebi.ac.uk/Tools/msa/muscle/>) with default parameters and adjusted manually in Mesquite²² prior to analysis. The data set consisted of 85 sequences and 559 characters, including the outgroup taxa. The data set was then analyzed using maximum likelihood in GARLI²⁶ employing the GTR+I+G model of evolution as determined by ModelTest,²⁷ followed by a bootstrap analysis with 1000 replicates. Based on preliminary results resolution of the tree was improved by filtering the alignment to include only 54 sequences, including those strains that appeared to be most closely related to FL2137. Following realignment and analysis as above, the strain was placed with strong support within the genus *Teratosphaeria* (Figure S1, Supporting Information). However, the analysis could not place the strain conclusively at the species level. Pending a morphological description, the strain was designated *Teratosphaeria* sp. FL2137. Sequence data for *Teratosphaeria* sp. FL2137 have been deposited in GenBank under accession number KX908743.1.

Cultivation and Isolation of Metabolites. Small-scale cultivation of the fungus *Teratosphaeria* sp. FL2137 in PDA, PDB, and PDB+Cu culture media gave the highest yield and cytotoxic activity for the EtOAc extract obtained from the PDB+Cu²⁺ culture medium. Thus, PDB+Cu²⁺ culture medium was chosen for large-scale cultivation of the fungus. A seed culture of *Teratosphaeria* sp. FL2137 grown on PDA for 2 weeks was used for inoculation. Mycelia were scraped out, vortexed with sterile PDB (90 mL), and filtered through a 100 μm sterile filter to separate very small fragments of hyphae from the mycelia. Absorbance of this suspension was measured at 600 nm and adjusted to 0.6. This suspension was used to inoculate $5 \times 2.0 \text{ L}$ Erlenmeyer flasks, each holding 1.0 L of PDB containing 0.25 mM CuSO_4 (PDB+Cu²⁺) and incubated at 160 rpm and 28°C . The glucose level of the medium was monitored using glucose strips (URISCAN glucose strips). After 4 weeks the glucose test indicated the absence of glucose in the medium. Mycelia were then separated by filtration, and the filtrate was extracted with EtOAc ($3 \times 2 \text{ L}$). The middle interface layer that existed between EtOAc and H_2O during the extraction was concentrated under reduced pressure to afford a dark brown solid (22.6 mg). Combined EtOAc extracts were washed with H_2O , dried over anhydrous Na_2SO_4 , and filtered. The filtrate was evaporated under reduced pressure to afford the crude EtOAc extract as a dark brown solid (767 mg). Both samples were subjected to cytotoxicity assay at a concentration of 10 $\mu\text{g}/\text{mL}$. Of these, only the sample obtained from the middle interface layer during the extraction exhibited cytotoxic activity. This sample (22.6 mg) was subjected to column chromatography (CC) over silica gel (15 g) made up in CHCl_3 and eluted with CHCl_3 to give metabolites **1** (1.7 mg) and **7** (6.9 mg). A portion (453.0 mg) of the crude EtOAc extract was subjected to CC over silica gel (12.5 g) made up in CH_2Cl_2 and eluted with CH_2Cl_2 (150 mL), 1% $\text{CH}_2\text{Cl}_2/\text{MeOH}$ (99:1) (150 mL), $\text{CH}_2\text{Cl}_2/\text{MeOH}$ (98:2) (100 mL), $\text{CH}_2\text{Cl}_2/\text{MeOH}$ (97:3) (100 mL), $\text{CH}_2\text{Cl}_2/\text{MeOH}$ (96:4) (100 mL), $\text{CH}_2\text{Cl}_2/\text{MeOH}$ (94:6) (100 mL), $\text{CH}_2\text{Cl}_2/\text{MeOH}$ (90:10) (100 mL), and finally MeOH (100 mL). A total of 180 fractions (5 mL each) were collected, and those having similar TLC profiles were combined to give 11 major fractions [A (1.9 mg), B (3.4 mg), C (20.2 mg), D (15.4 mg), E (10.9 mg), F (27.6 mg), G (32.6 mg), H (193.2 mg), I (44.4 mg), J (27.6 mg), and K (21.1 mg)]. Fraction A contained **1** in trace amounts, as revealed by TLC analysis. Fraction B (3.4 mg) was purified by preparative TLC (silica gel) eluting two times using CH_2Cl_2 to give an additional quantity of **7** (2.2 mg, R_f 0.3). Fraction C (20.0 mg) was separated by

preparative TLC (silica gel) using CH₂Cl₂/MeOH (98:2) as eluent to give five bands [C₁ (0.6 mg, R_f 0.9), C₂ (1.4 mg, R_f 0.8), C₃ (1.9 mg, R_f 0.6), C₄ (10.8 mg, R_f 0.5), and C₅ (3.3 mg, R_f 0.3)]. Band C₂ (1.4 mg) was further purified by preparative RP-HPLC (RP-18) using MeOH/H₂O (60:40) as the mobile phase (flow rate 2.0 mL/min) to give 4 (0.8 mg, t_R 30 min). Bands C₄ and C₅ obtained from above preparative TLC gave 2 (10.8 mg) and 3 (3.3 mg), respectively. Column fractions D and E were found to contain 2 and 6 as minor and major compounds, respectively. Fraction D also contained trace amounts of 4. Column fraction F was found to contain 6 (27.6 mg). Fraction G (13.3 mg) was separated by preparative TLC (silica gel) eluting five times using CH₂Cl₂/MeOH (96:4) as eluent to give an additional quantity of 3 (5.4 mg, R_f 0.7). Fraction H (10.0 mg) was purified by preparative TLC (silica gel) using CH₂Cl₂/MeOH (96:4) as eluent to provide an additional quantity of 3 (8.6 mg, R_f 0.5). Fraction I (44.4 mg) also contained 3 as the major compound. Column fraction J (19.2 mg) was separated by preparative TLC (silica gel) eluting five times using CH₂Cl₂/MeOH (96:4) as the eluent to give a fraction (11.2 mg, R_f 0.4), which on further purification by preparative RP-HPLC (RP-18) using MeOH/H₂O (25:75) as the mobile phase afforded 5 (4.0 mg, t_R 20 min).

Teratosphaerone A (1): orange, amorphous solid; UV (EtOH) λ_{max} (log ε) 218 (4.55), 268 (4.19), 427 (3.63) nm; IR (KBr) ν_{max} 1645, 1596, 1392, 1292, 1213, 1155, 970 cm⁻¹; ¹H and ¹³C NMR data, see Tables 1 and 2, respectively; positive HRESIMS m/z 241.0471 [M + Na]⁺ (calcd for C₁₂H₁₀O₄Na, 241.0477).

Teratosphaerone B (2): white, amorphous solid; [α]_D²⁵ +16.3 (c 0.86, CH₃OH); UV (EtOH) λ_{max} (log ε) 218 (4.07), 280 (3.93), 319 (3.60) nm; IR (KBr) ν_{max} 3429, 1627, 1301, 1207, 1155, 964 cm⁻¹; ¹H and ¹³C NMR data, see Tables 1 and 2, respectively; positive HRESIMS m/z 245.0786 [M + Na]⁺ (calcd for C₁₂H₁₄O₄Na, 245.0790).

Iso-balticol B (3): white, amorphous solid; [α]_D²⁵ +30.9 (c 1.14, MeOH); UV (EtOH) λ_{max} (log ε) 216.5 (4.00), 231.5 (3.84), 280 (3.97), 319 (3.64) nm; IR (KBr) ν_{max} 3400, 1625, 1301, 1265, 1205, 1157, 960 cm⁻¹; ¹H and ¹³C NMR data, see Tables 1 and 2, respectively; positive HRESIMS m/z 261.0732 [M + Na]⁺ (calcd for C₁₂H₁₄O₅Na, 261.0739).

Iso-balticol B-4,9-acetonide (4): white, amorphous solid; [α]_D²⁵ +12.3 (c 0.08, MeOH); UV (EtOH) λ_{max} (log ε) 216.5 (3.95), 232 (3.75), 278 (3.86), 320 (3.56) nm; IR (KBr) ν_{max} 1624, 1298, 1263, 1205, 1153, 966 cm⁻¹; ¹H and ¹³C NMR data, see Tables 1 and 2, respectively; positive HRESIMS m/z 301.1049 [M + Na]⁺ (calcd for C₁₃H₁₈O₅Na, 301.1052).

(+)-Balticol C (5): white, amorphous solid; [α]_D²⁵ +13.4 (c 0.30, MeOH); UV (EtOH) λ_{max} (log ε) 216.5 (4.09), 232 (3.92), 281 (4.05), 319 (3.73) nm; IR (KBr) ν_{max} 3400, 1631, 1298, 1159 cm⁻¹; ECD (MeOH) [θ] +2644 (236 nm), +5078 (277 nm); ¹H and ¹³C NMR data, see Tables 1 and 2, respectively; positive HRESIMS m/z 277.0673 [M + Na]⁺ (calcd for C₁₂H₁₄O₆Na, 277.0688).

(3aS,9R,9aS)-1(9a),3(3a),9-Hexahydromonosporascone (6): white, amorphous solid; [α]_D²⁵ +25.3 (c 0.49, MeOH); UV (EtOH) λ_{max} (log ε) 215 (4.06), 233 (3.87), 287 (4.08), 319 (3.73) nm; IR (KBr) ν_{max} 3332, 3236, 1622, 1276, 1245, 1205, 1132, 985 cm⁻¹; ¹H and ¹³C NMR data, see Tables 1 and 2, respectively; positive HRESIMS m/z 273.0738 [M + Na]⁺ (calcd for C₁₃H₁₄O₅Na, 273.0739).

Monosporascone (7): yellow, amorphous solid; negative APCIMS m/z 244 [M]⁻.

Methylation of 2, 3, and 6. To a solution of 2 (5.0 mg) in acetone (0.5 mL) were added Me₂SO₄ (25.0 μL) and K₂CO₃ (25.0 mg), and the mixture was refluxed at 80 °C for 1.5 h (TLC control). The reaction mixture was then filtered, and the filtrate evaporated under reduced pressure. The resulting crude product was purified by preparative TLC (silica gel) using CH₂Cl₂/MeOH (96:4) to afford 8 (2.4 mg, R_f 0.5). Methylation of 3 (5.0 mg) was also carried out using the same procedure described above. The resulting crude product was purified by preparative TLC (silica gel), developing two times using CH₂Cl₂/MeOH (96:4), to afford 9 (1.9 mg, R_f 0.2), 10 (1.4 mg, R_f 0.7), and 11 (0.6 mg, R_f 0.5). Methylation of 6 (5.0 mg) was also

carried out by the same procedure described above. The resulting crude product was purified by preparative TLC (silica gel), developing two times using CH₂Cl₂/MeOH (96:4), to afford 13 (3.7 mg, R_f 0.6).

8-O-Methylteratosphaerone B (8): white, amorphous solid; ¹H NMR data, see Supporting Information Table S2; ¹³C NMR data, see Supporting Information Table S3; positive APCIMS m/z 237 [M + H]⁺.

8-O-Methyl-iso-balticol B (9): white, amorphous solid; ¹H NMR data, see Supporting Information Table S2; ¹³C NMR data, see Supporting Information Table S3; positive APCIMS m/z 253 [M + H]⁺.

9-O-Methyl-iso-balticol B (10): white, amorphous solid; ¹H NMR data, see Supporting Information Table S2; ¹³C NMR data, see Supporting Information Table S3; negative APCIMS m/z 251 [M + H]⁺.

8,9-Di-O-methyl-iso-balticol B (11): white, amorphous solid; ¹H NMR data, see Supporting Information Table S2; ¹³C NMR data, see Supporting Information Table S3; positive APCIMS m/z 267 [M + H]⁺.

5-O-Methyl-(3aS,9R,9aS)-1(9a),3(3a),9-hexahydromonosporascone (13): white, amorphous solid; ¹H NMR data, see Supporting Information Table S2; ¹³C NMR data, see Supporting Information Table S3; positive APCIMS m/z 265 [M + H]⁺.

Acetylation of 6. To a solution of 6 (5.0 mg) in pyridine (0.2 mL) was added Ac₂O (5.0 μL), and the mixture was stirred at 25 °C for 24 h (TLC control). Pyridine and excess Ac₂O were evaporated under reduced pressure and by azeotroping with EtOH. The resulting crude product was purified by preparative TLC (silica gel), developing two times using CH₂Cl₂/MeOH (98:2), to afford 12 (5.3 mg, R_f = 0.63).

5,9-Di-O-acetyl-(3aS,9R,9aS)-1(9a),3(3a),9-hexahydromonosporascone (12): white, amorphous solid; ¹H NMR data, see Supporting Information Table S2; ¹³C NMR data, see Supporting Information Table S3; positive APCIMS (+) m/z 335 [M + H]⁺, 367 [M + H + CH₃OH]⁺, 307 [(M + H + CH₃OH) - CH₃COOH]⁺.

Preparation of Acetonide of 3. To a solution of 3 (5.0 mg) in acetone (2.5 mL) was added *p*-TsOH (2.0 mg), and the mixture was stirred at room temperature for 7 days. Saturated aqueous NaHCO₃ (2.5 mL) was then added, and the reaction mixture was extracted with EtOAc (2.5 mL × 3). Combined EtOAc extracts were washed with H₂O, dried over anhydrous Na₂SO₄, and filtered. The filtrate was evaporated under reduced pressure, and the crude product obtained was purified by preparative TLC (silica gel) using CH₂Cl₂/MeOH (98:2) to give a product (1.0 mg, R_f 0.7) identical (LR-MS, ¹H and ¹³C NMR spectra) to 4.

Preparation of (S)- and (R)-MTPA Esters of 8. Compound 8 (1.5 mg) was transferred into an NMR tube (5.0 mm) and dried completely under vacuum. Pyridine-*d*₅ (0.3 mL) was then added into the NMR tube. After obtaining the ¹H NMR spectrum, (R)-(-)-MTPA-Cl (5.0 μL) was added into the NMR tube under a stream of N₂. The NMR tube was carefully shaken and was left at 25 °C while monitored by ¹H NMR. After 14 h the reaction mixture was transferred into a round-bottom flask. Pyridine was evaporated under reduced pressure and by azeotroping with EtOH. The resulting crude product was purified by preparative TLC (silica gel) using CH₂Cl₂/MeOH (97:3) as the eluent to give (S)-MTPA ester derivative 8a (2.2 mg, R_f 0.7). ¹H NMR (400 MHz, CDCl₃) data were assigned on the basis of the correlations of ¹H-¹H COSY, HSQC, and HMBC spectra: δ 6.577 (1H, d, J = 2.4 Hz, H-5), 6.457 (1H, d, J = 2.4, H-7), 6.106 (1H, s, H-4), 2.548 (3H, m, H₂-2 and H-3), 1.047 (3H, d, J = 6.0 Hz, H₃-9).

Another portion of compound 8 (1.5 mg) was reacted with (S)-(+)-MTPA-Cl (5.0 μL) according to the same procedure described above. After the workup, the resulting crude product was purified by preparative TLC (silica gel) using CH₂Cl₂/MeOH (97:3) to afford (R)-MTPA ester derivative 8b (2.1 mg, R_f 0.5): ¹H NMR (400 MHz, CDCl₃) δ 6.643 (1H, s, H-5), 6.501 (1H, s, H-7), 6.097 (1H, s, H-4), 2.506 (3H, m, H₂-2 and H-3), 0.941 (3H, d, J = 4.8 Hz, H₃-9).

Preparation of (S)- and (R)-MTPA Esters of 11. Following the same procedure described for the preparation of 8a and 8b, portions (1.0 mg each) of 11 were reacted in two NMR tubes with (R)-

(-)-MTPA-Cl (5 μ L) and (S)-(+)-MTPA-Cl (5.0 μ L) separately at 25 °C for 14 h using pyridine-*d*₅ (0.3 mL) as the solvent. After workup, resulting crude products were purified by preparative TLC (silica gel) using CH₂Cl₂/MeOH (97:3) to afford (S)-MTPA and (R)-MTPA ester derivatives **11a** (1.46 mg, R_f 0.7) and **11b** (1.40 mg, R_f 0.6), respectively.

(S)-MTPA Ester Derivative (**11a**): ¹H NMR (400 MHz, CDCl₃) δ 6.723 (1H, d, J = 2.3 Hz, H-5), 6.489 (1H, d, J = 2.3 Hz, H-7), 6.224 (1H, d, J = 1.9 Hz, H-4), 4.045 (2H, m, H-9), 2.779 (1H, m, H-3), 2.517 (2H, m, H-2).

(R)-MTPA Ester Derivative (**11b**): ¹H NMR (400 MHz, CDCl₃) δ 6.767 (1H, d, J = 2.3 Hz, H-5), 6.512 (1H, d, J = 2.3 Hz, H-7), 6.285 (1H, d, J = 1.9 Hz, H-4), 3.136 (1H, dd, J = 9.2, 5.4 Hz, H-9a), 3.061 (1H, t, J = 9.2 Hz, H-9b), 2.626 (1H, m, H-3), 2.442 (2H, m, H-2).

Preparation of (S)- and (R)-MTPA Esters of 13. Following the same procedure described for **8a** and **8b**, portions (1.5 mg each) of **13** were reacted in two NMR tubes with (R)-(-)-MTPA-Cl (5 μ L) and (S)-(+)-MTPA-Cl (5.0 μ L) separately at 25 °C for 14 h using pyridine-*d*₅ (0.3 mL) as the solvent. After the workup, resulting crude products were purified by preparative TLC (silica gel) using CH₂Cl₂/MeOH (97:3) to afford (S)-MTPA and (R)-MTPA ester derivatives **13a** (2.1 mg, R_f 0.6) and **13b** (2.2 mg, R_f 0.7), respectively.

(S)-MTPA Ester Derivative (**13a**): ¹H NMR (400 MHz, CDCl₃) δ 6.402 (1H, d, J = 2.2 Hz, H-6), 6.355 (1H, d, J = 4.6 Hz, H-9), 6.312 (1H, d, J = 2.2 Hz, H-8), 4.062 (1H, dd, J = 9.0, 7.5 Hz, H-3), 3.954 (1H, dd, J = 9.0, 4.2 Hz, H-3), 3.863 (1H, dd, J = 9.0, 8.1 Hz, H-1), 3.678 (1H, dd, J = 9.0, 6.3 Hz, H-1), 3.269 (1H, m, H-3a), 3.213 (1H, m, H-9a).

(R)-MTPA Ester Derivative (**13b**): ¹H NMR (400 MHz, CDCl₃) δ 6.459 (1H, d, J = 1.6 Hz, H-8), 6.439 (1H, d, J = 1.6 Hz, H-6), 6.239 (1H, d, J = 4.3 Hz, H-9), 4.055 (1H, dd, J = 8.7, 7.8 Hz, H-3), 3.802 (1H, dd, J = 8.7, 5.6 Hz, H-3), 3.788 (1H, dd, J = 9.3, 2.2 Hz, H-1), 3.497 (1H, dd, J = 9.3, 6.1 Hz, H-1), 3.259 (1H, m, H-3a), 3.194 (1H, m, H-9a).

Cytotoxicity Assay. The resazurin-based colorimetric (Almar Blue) assay was used as described previously¹⁸ for evaluating *in vitro* cytotoxicity of metabolites **1** and **7** against human non-small-cell lung (NCI-H460), human CNS glioma (SF-268), human breast (MCF-7), metastatic human prostate adenocarcinoma (PC-3M), and human breast adenocarcinoma (MDA-MB-231) cancer cell lines. Doxorubicin and DMSO were used as positive and negative controls, respectively. All experiments were performed in triplicate.

■ ASSOCIATED CONTENT

Supporting Information

The Supporting Information is available free of charge on the ACS Publications website at DOI: 10.1021/acs.jnatprod.7b00838.

¹H, ¹³C, HSQC, and HMBC NMR spectra of **1–6** and **8–10**, ¹H and ¹³C NMR spectra of **11–13**, ¹H–¹H COSY spectra of **3**, **4**, and **6**, 1D NOESY spectra of **2–4** and **13**, ROESY spectrum of **5**, tables of ¹H and ¹³C NMR spectroscopic data of **8–13**, ECD spectra of **2–6**, and results of phylogenetic analyses confirming placement of the fungus FL2137 within the genus *Teratosphaeria* (PDF)

■ AUTHOR INFORMATION

Corresponding Author

*Tel: (520) 621-9932. Fax: (520) 621-8378. E-mail: leslieg1@email.arizona.edu.

ORCID

A. A. Leslie Gunatilaka: 0000-0001-9663-3600

Notes

The authors declare no competing financial interest.

■ ACKNOWLEDGMENTS

Financial support for this work was provided by Grant R01 CA090265 funded by the National Cancer Institute (NCI, NIH) and Grant P41 GM094060 funded by National Institute of General Medical Sciences (NIGMS, NIH). We thank the Fulbright Visiting Scholar Program, Council for International Exchange of Scholars, Institute of International Education, Washington, D.C., for awarding a Fulbright Fellowship to C.P., and Prof. Lijiang Xuan of Center for Modernization of TCM, Shanghai Institute of Materia Medica, PR China, for obtaining HRESIMS data.

■ DEDICATION

Dedicated to Dr. Susan Band Horwitz, of Albert Einstein College of Medicine, Bronx, NY, for her pioneering work on bioactive natural products.

■ REFERENCES

- (1) (a) Gunatilaka, A. A. L. *J. Nat. Prod.* **2006**, *69*, 509–526. (b) Kusari, S.; Spiteller, M. *Nat. Prod. Rep.* **2011**, *28*, 1203–1207. (c) Zheng, C.-J.; Li, L.; Zou, J.-P.; Han, T.; Qin, L.-P. *Pharm. Biol.* **2012**, *50*, 129–133.
- (2) (a) Saikkonen, K. *Fungal Biol. Rev.* **2007**, *2*, 67–74. (b) Sieber, T. N. *Fungal Biol. Rev.* **2007**, *2*, 75–89. (c) Promptuta, L.; Lumyong, S.; Dhanasekaren, V.; McKenzie, E. H. C.; Hyde, K. D.; Jeewon, R. *Microb. Ecol.* **2007**, *53*, 579–590.
- (3) (a) Luo, J.-G.; Wang, X.-B.; Xu, Y.; U'Ren, J. M.; Arnold, A. E.; Kong, L.-Y.; Gunatilaka, A. A. L. *Org. Lett.* **2014**, *16*, 5944–5947. (b) Xu, Y.-M.; Mafezoli, J.; Oliveira, M. C. F.; U'Ren, J. M.; Arnold, A. E.; Gunatilaka, A. A. L. *J. Nat. Prod.* **2015**, *3*, 2738–2747. (c) Wijeratne, E. M. K.; Gunaherath, G. M. K. B.; Chapla, V. M.; Tillotson, J.; Cruz, F. d. I.; Kang, M.-J.; U'Ren, J. M.; Araujo, A. R.; Arnold, A. E.; Chapman, E.; Gunatilaka, A. A. L. *J. Nat. Prod.* **2016**, *79*, 2738–2747. (d) Luo, J.-G.; Xu, Y.-M.; Sandberg, D. C.; Arnold, A. E.; Gunatilaka, A. A. L. *J. Nat. Prod.* **2017**, *80*, 76–81. (e) Gubiani, J. R.; Wijeratne, E. M. K.; Shi, T.; Araujo, A. R.; Arnold, A. E.; Chapman, E.; Gunatilaka, A. A. L. *Bioorg. Med. Chem.* **2017**, *25*, 1860–1866. (f) Bashyal, B. P.; Wijeratne, E. M. K.; Tillotson, J.; Arnold, A. E.; Chapman, E.; Gunatilaka, A. A. L. *J. Nat. Prod.* **2017**, *80*, 427–433.
- (4) Crous, P. W.; Summerell, B. A.; Mostert, L.; Groenewald, J. *Persoonia.* **2008**, *20*, 59–86.
- (5) Ganley, R. J.; Brunfeldt, S. J.; Newcombe, G. *Proc. Natl. Acad. Sci. U. S. A.* **2004**, *101*, 10107–10112.
- (6) Crous, P. W.; Braun, U.; Groenewald, J. Z. *Stud. Mycol.* **2007**, *58*, 1–32.
- (7) Paranagama, P. A.; Wijeratne, E. M. K.; Burns, A. M.; Marron, M. T.; Gunatilaka, M. K.; Arnold, A. E.; Gunatilaka, A. A. L. *J. Nat. Prod.* **2007**, *70*, 1700–1705.
- (8) Stipanovic, R. D.; Zhang, J.; Bruton, B. D.; Wheeler, M. H. J. *Agric. Food Chem.* **2004**, *52*, 4109–4112.
- (9) Thines, E.; Anke, H. *J. Antibiot.* **1998**, *51*, 387–393.
- (10) Shushni, M. A. M.; Mentel, R.; Lindequist, U.; Jansen, R. *Chem. Biodiversity* **2009**, *6*, 127–137.
- (11) Zhou, Y.-H.; Zhang, M.; Zhu, R.-X.; Zhang, J.-Z.; Xie, F.; Li, X.-B. *J. Nat. Prod.* **2016**, *79*, 2149–2157.
- (12) Fujimoto, H.; Okuyama, H.; Yoshida, E.; Yamazaki, M. *Mycotoxins* **1995**, *41*, 61–66.
- (13) Whyte, A. C.; Gloer, K. B.; Gloer, J. B.; Koster, B.; Malloch, D. *Can. J. Chem.* **1997**, *75*, 768–772.
- (14) Medentsev, A. G.; Akimenko, V. K. *Phytochemistry* **1998**, *47*, 935–959.
- (15) (a) Ohtani, I.; Kusumi, T.; Kashman, Y.; Kakisawa, H. *J. Am. Chem. Soc.* **1991**, *113*, 4092–12096. (b) Kusumi, T.; Ohtani, I.; Inouye, Y.; Kashman, Y.; Kakisawa, H. *Tetrahedron Lett.* **1998**, *37*, 4731–4734.
- (16) (a) Arango, V.; Robledo, S.; Séon-Ménial, B.; Figadère, B.; Cardona, W.; Sáez, J.; Otaño, F. *J. Nat. Prod.* **2010**, *73*, 1012–1014.

- (b) Shao, C.-L.; Wu, H.-X.; Wang, C.-Y.; Liu, Q.-A.; Xu, Y.; Wei, M.-Y.; Qian, P.-Y.; Gu, Y.-C.; Zheng, C.-J.; She, Z.-G.; Lin, Y.-C. *J. Nat. Prod.* **2011**, *74*, 629–633. (c) Yu, J. S.; Moon, E.; Choi, S. U.; Kim, K. H. *Tetrahedron Lett.* **2016**, *57*, 1699–1701.
- (17) (a) Bringmann, G.; Munchbach, M.; Messer, K.; Koppler, D.; Michel, M.; Schupp, O.; Wenzel, M.; Louis, A. M. *Phytochemistry* **1999**, *51*, 693–699. (b) Bringmann, G.; Messer, K.; Saeb, W.; Peters, E. M.; Peters, K. *Phytochemistry* **2001**, *56*, 387–391.
- (18) (a) O'Brien, J.; Wilson, I.; Orton, T.; Pognan, F. *Eur. J. Biochem.* **2000**, *267*, 5421–5426. (b) Wijeratne, E. M. K.; Bashyal, B. P.; Liu, M. X.; Rocha, D. D.; Gunaherath, G. M. K. B.; U'Ren, J. M.; Gunatilaka, M. K.; Arnold, A. E.; Whitesell, L.; Gunatilaka, A. A. L. *J. Nat. Prod.* **2012**, *3*, 361–369.
- (19) U'Ren, J. M.; Arnold, A. E. *PeerJ* **2016**, *4*, e2768.
- (20) Ewing, B.; Green, P. *Genome Res.* **1998**, *8*, 186–194.
- (21) Ewing, B.; Hillier, L.; Wendl, M. C.; Green, P. *Genome Res.* **1998**, *8*, 175–185.
- (22) Maddison, W. P.; Maddison, D. R. *Mesquite*. 2011; www.mesquiteproject.org.
- (23) Altschul, S. F.; Gish, W.; Miller, W.; Myers, E. W.; Lipman, D. J. *J. Mol. Biol.* **1990**, *215*, 403–410.
- (24) Liu, K. L.; Porrás-Alfaro, A.; Kuske, C. R.; Eichorst, S. A.; Xie, G. *Appl. Environ. Microbiol.* **2012**, *78*, 1523–1533.
- (25) Taylor, K.; Andjic, V.; Barber, P. A.; Hardy G, E. J.; Burgess, T. I. *Mycol. Prog.* **2012**, *11*, 159–169.
- (26) Zwickl, D. J. Genetic algorithm approaches for the phylogenetic analysis of large biological sequence datasets under the maximum likelihood criterion. Ph.D. Dissertation, The University of Texas at Austin, Austin, TX, 2008; pp 1–114.
- (27) Posada, D.; Crandall, K. A. *Bioinformatics* **1998**, *14*, 817–818.